Performance Tests of a Permanent Magnet Thrust Bearing for a Hydropower Synchronous Generator Test-Rig

J. José Pérez-Loya, C. Johan D. Abrahamsson, Fredrik Evestedt, and Urban Lundin

Division of Electricity, Department of Engineering Sciences
Uppsala University, Uppsala, SE75121, Sweden
Jose@Angstrom.uu.se, Johan.Abrahamsson@Angstrom.uu.se, Fredrik.Evestedt@Angstrom.uu.se,
Urban.Lundin@Angstrom.uu.se

Abstract ─ Permanent magnets are an attractive material to be utilized in thrust bearings as they offer relatively low losses. If utilized properly, they have a long service lifetime and are virtually maintenance free. In this contribution, we communicate the results of the tests performed on a permanent magnet thrust bearing that was custom built and installed in a hydropower synchronous generator test-rig. Tridimensional finite element simulations were performed and compared with measurements of axial force. Spin down times and axial force ripple have also been measured. We found good correspondence between the measurements and the simulations.

Index Terms ─ Axial bearing, Halbach array, hydropower, magnetic bearing, permanent magnet, thrust bearing.

I. INTRODUCTION

A. Background

Large electromagnetic actuators have been used successfully since the 1950's to partly bear the load of vertical hydropower units [1]. This places hydropower among the oldest applications of magnetic thrust bearings. Even though, the technology improves the reliability and efficiency of the thrust system, their utilization is not widespread. They have been mostly utilized in pump storage stations. Notably, as a problem solver in Europe's largest installation of this type at Dinorwig in the United Kingdom [2]. In general, as often happens with industrial components, thrust bearings for hydropower are required to be technically superior compared to the past. They are required to have a higher degree of efficiency, to operate with a higher level of reliability, to be more sustainable and to bear larger loads, both static and transient. They also need to operate in tougher conditions, the generation patterns required by energy markets and the introduction of intermittent solar and wind power results in an increased number of start and stop operations. Moreover, in some occasions, the generators are required to operate at a peak level, or on the contrary at low capacity. This operational patterns cause extra wear and tear in the thrust bearing pads. When it comes to reliability, a high percentage of the generator failures in large machines are due to bearing failures [3, 4, 5]. According to an analysis performed in 1980, more than half of the operational failures of equipment in hydropower stations is due to unreliable operation of the thrust bearing [6]. The economic implications of such failures are large. Not only due to the expenses required to repair the machine, but also due to production loss. On top of this, some utilities are looking for strategies to eliminate oil in the hydropower stations in order to eliminate the risk of pollution in the rivers. To achieve this objective relatively small hydropower generators have been fully levitated [7]. When it comes to large installations, thrust bearings are at its limit. Increasing their size to increase their capacity is not an easy task as the losses depend on the diameter of the bearing. With mechanical solutions, installing more than one bearing in order to increase the load capacity is not an option for machines in hydropower sizes. One way to cope with these challenges is to use magnetic forces either from electromagnets, permanent magnets or a combination of both [8], bearing the force only by magnetic means or in combination with mechanical bearings in a similar fashion as it has been done since the 1950's, but with 65 years of advances in crucial technology in relevant areas, such as control, electronics and magnetic materials. At Uppsala University a synchronous generator hydropower test-rig with magnetic bearings has been designed at constructed. The test-rig is flexible enough to allow the study of the behavior of the machine while operating on a permanent magnet thrust bearing, an electromagnetic thrust bearing, a roller thrust bearing or any combination of them. With these new tools, the advantages of utilizing magnetic forces in the thrust system can be further investigated.

The focus of this paper is on the performance and finite element simulations of a permanent magnet thrust bearing constructed with 2532 N48 Nd-Fe-B permanent magnets in a Hallbach array. The permanent magnet thrust bearing, is the preferred bearing for the test-rig as it does not require external power or control to function

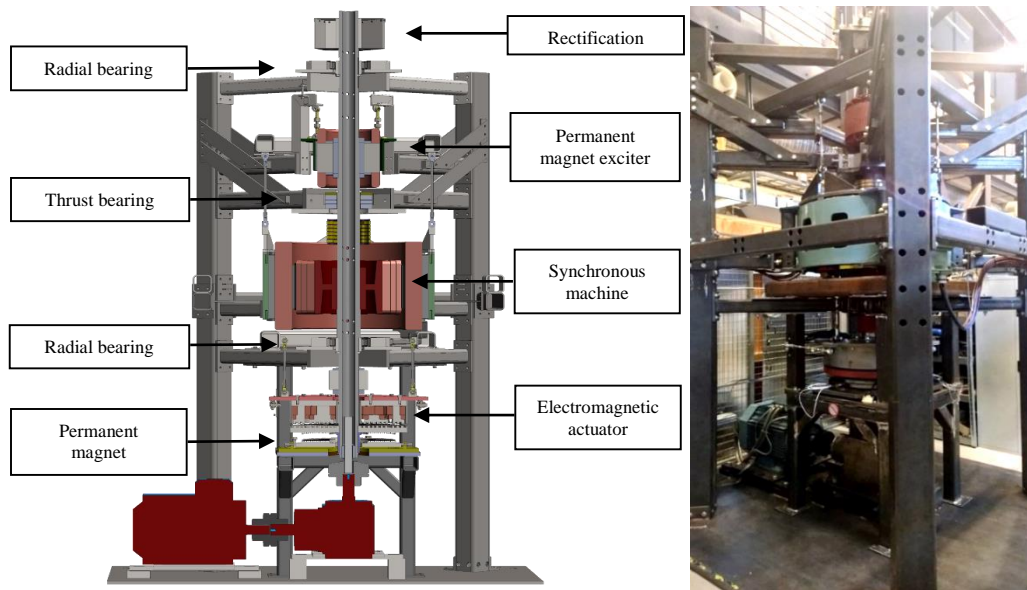and it offers lower losses compared to its mechanical   counterpart.

Fig. 1. (Left) Cross sectional view of the 3D CAD model of the vertical synchronous generator test-rig built and designed at Uppsala University. (Right) Actual test rig.

B. Brief description of the experimental test-rig

The vertical synchronous generator test-rig built and designed by the hydropower group at Uppsala University as described by Wallin, [9] has been upgraded to accommodate a range of features. As shown in Fig. 1, from bottom to top, some of them are: a permanent magnet thrust bearing, an electromagnetic actuator and a brushless excitation system with permanent magnets [10]. The machine was also equipped with a roller thrust bearing that was mounted between the generator and the brushless exciter. After the upgrades, the shaft resulted in a weight of 12.56 kN. The rotational speed needed to synchronize the machine with the grid is 500 rpm. To mimic the power exerted by water on a turbine, an induction motor and a gearbox were utilized, they can be seen in Fig. 1 (left) in dark red. The torque was transferred from the gearbox to the shaft of the test rig through a flexible coupling and a ball spline, these components can be seen in Fig. 2 (top). This construction allowed us to adjust the axial position of the shaft in relation to the static parts without affecting the torque transfer. The idea was to be able to use the machine while resting on the permanent magnet thrust bearing, the roller bearing, while utilizing the electromagnet actuator or as well as any possible combination between them. The actual adjustment of the axial position of the shaft was realized by moving the permanent magnet thrust bearing up and down. When the permanent magnet thrust bearing sat at its lowest position, the shaft descended to rest on the mechanical bearing. In this position, the

airgap of the permanent magnet thrust bearing was so large that there was virtually no force exerted on the shaft by the permanent magnets. On the contrary, as the permanent magnet thrust bearing was moved up, the magnetic forces started to push on the shaft. If raised enough, the shaft could be released from the mechanical bearing and rest only on the permanent magnets, all the experiments reported in this paper were performed with the test-rig in this position, except the spin down test on the mechanical bearing. When resting on the magnetic thrust bearing, the shaft is stable in the axial direction but unstable in the radial direction. This phenomena can be described by extension of Earnshaw's theorem for electrostatic charges [11]. For this reason, the shaft was held in the radial direction by two radial roller bearings. They sit under the control and rectification box and under the generator respectively. To allow them to function properly regardless of the axial position chosen, the shaft was provisioned with oversized inner races. In this way contact between the rollers and a proper inner race was always achieved. The designation of both radial bearings selected is NU 326 ECP, the inner races belong to NU 2326 ECMA, all from SKF.

C. Permanent magnet thrust bearing

The device was designed and custom built as part of a major upgrade to the test rig. The estimated weight of the rotating parts at the design stage was around 15 kN. The bearing was to be built by hand. Magnets that could be easily and safely handled by a person with no special

equipment were needed. For this practical reasons, it was decided to utilize cubic 12 mm N48 Nd-Fe-B permanent magnets. In order to accommodate as much magnetic material as possible in a given volume, a Hallbach array arranged in the radial direction was selected, 13 rows of magnets with alternating polarity were mounted to create a homo polar array in the angular direction. For practical and economic reasons it was convenient to utilize cubic magnets. However, the segmentation of the array carried its own drawbacks. One of them was that it could generate axial force ripple as the shaft rotates. There is at least one technique to prevent, or at least reduce this inconvenience. It involves covering the magnets with a thin piece of ferromagnetic material to smoothen out the field across the segmentation [12]. For this bearing, we decided to install a different number of magnets in the rotor than in the stator. Each of the rows of magnets have one pair of magnets difference than its counterpart in the other plate. By doing this, a constant overlap of magnetic material was achieved even when the shaft was rotated. Another measure taken to prevent force oscillations was to randomly position the rows of magnets in the angular direction in relation to each other. The resulting pattern of this efforts in the rotor plate is shown in Fig. 2. The details of the construction of the bearing can be found in [13]. Another drawback of this construction was that in order to evaluate the force capabilities of the bearing including the effect of the segmentation full 3D Finite element simulations were needed. The existent analytical formulas [8] or 2D simulations were not capable of evaluating the axial force ripple caused by the segmentation.

Fig. 2. (Top) Flexible coupling and driving end of the shaft. (Bottom) Permanent magnet thrust bearing rotor prior assembly. The details of the segmentation of the magnetic material can be appreciated.

II. METHOD

To be able to assess the performance of the bearing, we performed finite element simulations, axial force and axial force ripple measurements, and spin down tests.

A. Three dimensional finite element simulations

In order to take into account the segmentation in the bearing, we have simulated it using 3D FEM static simulations. For all of them, we used 2535 volumes. One for each magnet, one for a cylindrical portion of air between the permanent magnet surfaces that was basically the airgap, and two more for the air surrounding the magnets in the radial direction. Since a Hallbach array was utilized, we decided not to model the steel plates in which the magnets were mounted as the field in this region was expected to be relatively low. We started the simulation routine by importing the geometry from a dedicated CAD software (Solid Works 2015) into a commercial finite element program (Comsol 5.1). After the geometry was processed, we proceeded to mesh the cylindrical volume that represented the airgap. In this part of the procedure, we required 5 tetrahedral elements in the axial direction as it is the main region of interest. Afterwards, the mesh that resulted in the interface between the airgap and the magnet assembly was swept to discretize the remaining bodies, for each of them we utilized two elements in the axial direction, thus it resulted in pentahedral elements. With this meshing procedure, it was possible to take into account the segmentation of magnetic material in the permanent magnet thrust bearing assembly. One of the resulting meshes is shown in Fig. 3.

The resulting number of degrees of freedom solved for each mesh are shown in Table 1. As it can be seen, the number of degrees of freedom increases when the airgap is reduced. The reason is that we decided to utilize 5 elements in the axial direction to model the airgap. Therefore, the resulting number of elements varied with the airgap length. For a smaller airgap, the maximum size of the element was reduced, resulting in a larger number of mesh elements.
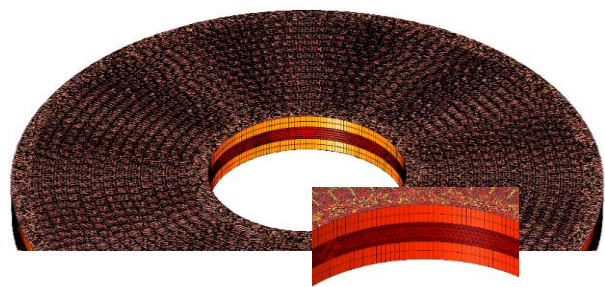

Fig. 3. One of the meshes utilized to calculate the force in the permanent magnet thrust bearing with the finite element method.

Table 1: Number of degrees of freedom solved for each simulation depending on the airgap length

Airgap (mm)	Number of Degrees of Freedom Solved
10	2.7756e7
11	2.5157e7
12	1.9514e7
13	1.7788e7
14	1.6306e7
15	1.4765e7
16	1.1542e7

After the meshing was performed, we proceeded to set the finite element formulation. We utilized the following constitutive relation for all the simulated volumes:

$$\mathbf{B} = \mu_0 \mu_r \mathbf{H} + \mathbf{B}_r . \qquad (1)$$

For the two volumes surrounding the magnets and the volume that represented the airgap, the relative permeability was set to $\mu_r = 1$. Since the grade of Nd-Fe-B permanent magnet material selected had a relatively high coercivity and the height to width aspect ratio of the magnets selected was high [14], we considered that implementing the $\mathbf{BH}$ curve of the magnets was not needed. Therefore, we set the relative permeability of the permanent magnet material to $\mu_r = 1.037$ and the remanence to $\mathbf{B}_r = 1.35\mathrm{T}$. The typical remanence for this batch of magnets was obtained directly from the manufacturer (Sura magnets), and the permeability from the datasheet of a typical N48 permanent magnet from Arnold magnetics [15]. The direction of magnetization of the permanent magnets was set according to the schematic shown in Fig. 4.

↓	←	↑	→	↓	←	↑	→	↓	←	↑	→	↓

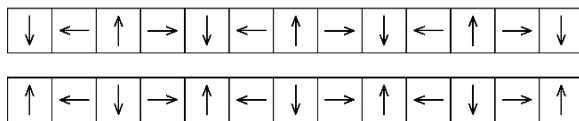| ↑	←	↓	→	↑	←	↓	→	↑	←	↓	→	↑

Fig. 4. Direction of magnetization utilized in the Hallbach arrays of the permanent magnet thrust bearing.

Afterwards, we solved for the magnetic vector potential using the following equation form:

$$\nabla \times (\mu_0^{-1} \mu_r^{-1} (\mathbf{B} - \mathbf{B}_r)) = \mathbf{0} , \qquad (2)$$

where:

$$\mathbf{B} = \nabla \times \mathbf{A} . \qquad (3)$$

In all the studies, the forces between the volumes that represented the stator and the rotor of the permanent magnet thrust bearing were calculated using the Maxwell stress tensor. In total, we performed 7 simulations at different airgaps to evaluate the force as the plates approached each other and 38 simulations at 16 mm airgap for different rotational positions between the

plates. 5 simulations in steps of 1 degree, 18 simulations in steps of 2 degrees, and 15 in steps of 5 degrees. With this amount of simulations we were able to cover one third a revolution. This was done to evaluate the axial force ripple as the bearing rotated.

B. Thrust vs. distance measurements

The measurements of thrust and distance between the bearing plates were taken in situ, with the bearing installed in the machine. We started by measuring the load exerted by the weight of the shaft on the bearing and the distance between the rotor and the stator. Afterwards, we artificially increased the load in the bearing as described in Fig. 5. To evaluate the axial force, three load cells were inserted in parallel under the bearing. The load cells used are of the doughnut type, model LTH350 from the company Futek. They were previously calibrated and the signals were properly amplified. We measured the airgap between the plates manually with a caliper at different points around the circumference of the bearing and then calculated the average.

C. Spin down tests

The test rig was provisioned with speed sensors that made it possible to evaluate the rotational speed of the machine over time during spin-down. The machine was accelerated to one third of the rated speed, afterwards the driving power was disconnected, the rotational speed was recorded when the machine was resting on the permanent magnet thrust bearing as well as when it was resting on the roller bearings.
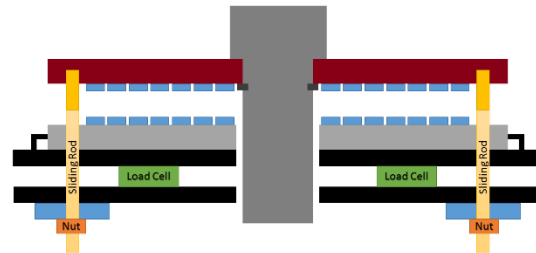

Fig. 5. Schematic of the axial force test set-up. Sliding rods (yellow) were attached to the rotor plate (red). Torque was applied to the nuts (orange), through washers (blue) that pressed on the static foundation that holds the bearing (black). By reaction, the rotor plate (red) was pulled downwards. The sliding rods were used to maintain the radial placement of the plates. To reduce their influence on the measurements, they were properly greased. The distance measurements between the plates were taken manually with a caliper, the force measurements were recorded with load cells (green).

D. Axial force ripple measurements

In order to evaluate the movement of the shaft in the axial direction, we measured the relative position

between the rotor and the stator with a high accuracy Eddy-current sensor from MICRO-EPSILON model eddyNCDT3010,S2. We did it at 500 rpm, the rated speed. At the same, we recorded the force measured in the three load cells that were described in Section II-B.

III. RESULTS AND DISCUSSIONS

The results arising from the methods presented are summarized in this section. The finite element method calculations are compared with the measurements performed for the thrust vs. distance and the axial force ripple.
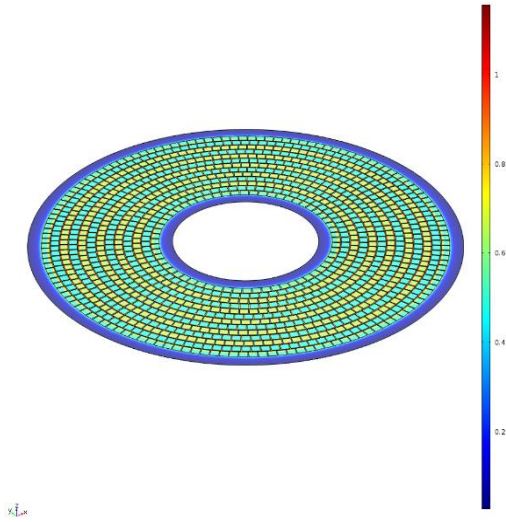

Fig. 6. Simulated flux density in the surface of one the permanent magnet bearing plates at an airgap of 16 mm. In order to be able to simulate the effects of the segmentation of the magnetic material, three-dimensional simulations were performed. In the figure, the flux density distribution pattern of the Hallbach array can be appreciated.

A. Thrust vs. distance measurements and finite element calculations

As described in the previous section, the permanent magnet thrust bearing was loaded from its usual load (shaft weight), to a value just under the maximum that the load cells could take. We also simulated the bearing in the same range. The resulting simulated magnetic flux density at the surface of one of the plates of the magnetic bearing is shown in Fig. 6. The calculated force between the plates at different airgaps with the three dimensional simulations and its corresponding measurements are shown in Fig. 7. We found good correspondence between them. In all the cases, the simulations showed a slight overestimation of the force. The discrepancy increased as the airgap was reduced. This is most likely due to the effects that we had chosen to neglect in order to simplify

the simulations, mainly the full magnetic characteristics of the permanent magnets and the steel plates in which the magnets were assembled. If both were implemented, it is expected that the force calculated would be lower as the plates approach each other. This is due to the fact that the leakage field on the plates will result in a small attractive force. On the other hand, the magnetic domains would deviate from ideal as the magnets are pushed closer. Both effects act in detriment of the repulsive force. Nevertheless, as we suspected, the influence of this simplifications were small. On the practical side, during the measurements, the assembly was constrained radially not only by the sliding rods utilized to exert and extra force on the bearing, but also by the radial bearings and the spline. They certainly had an effect on the measured forces, but as it can be appreciated from the comparison this effect was small as well.
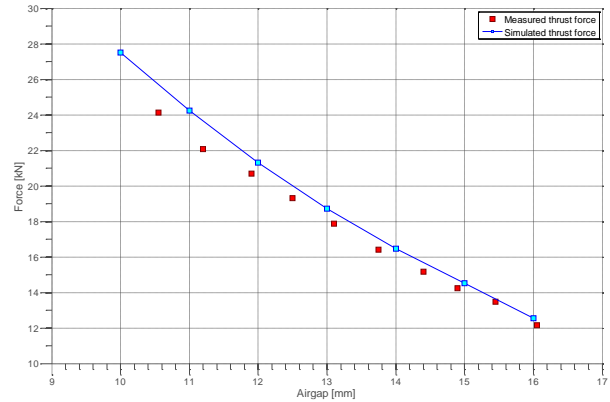

Fig. 7. Simulated and measured thrust forces as a function of airgap length.

B. Spin down tests

After the installation of the permanent magnet thrust bearing into the hydropower test-rig, a number of spin-down tests were made. These tests were performed with the rotor resting axially only on the permanent magnet thrust bearing, and also when it was supported only by the mechanical roller bearing. The rotor was accelerated to a rotational speed of 166.7 rpm, one third of the rated speed of the test-rig. The drive was thereafter turned off, and the rotor allowed to spin-down. The measured rotational speed over time for the two cases can be found in Fig. 8. From the figure it can be concluded that the losses in the machine when it is supported by the permanent magnet thrust bearing are lower that when it is supported by its mechanical counterpart. It is hard to isolate the losses of each thrust bearing from the losses in the other parts of the system, but if it is assumed that windage and radial bearing losses are the same for both tests, the difference presented in Fig. 8 corresponds to the difference in losses between both bearings.
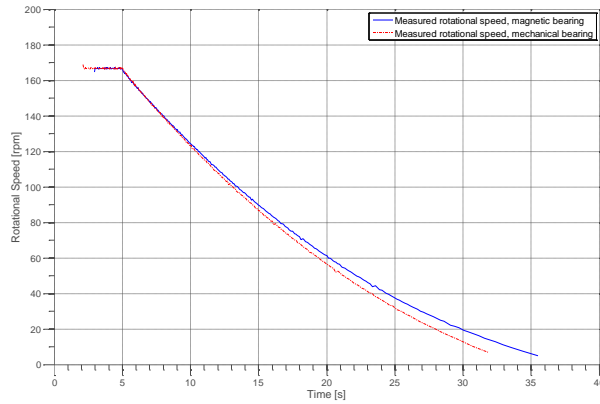
Fig. 8. Measured rotational speed as function of time during a spin-down test from a rotational speed of 166.7 rpm when the shaft was supported by the permanent magnet thrust bearing and the corresponding set of measurements when it was carried by a roller bearing.

C. Axial ripple measurements and finite element calculations

In order to estimate the influence that the segmentation of the magnetic material utilized to build the Hallbach arrays for the magnetic bearing as it rotates, we performed a large number of static simulations along one third of a revolution at an airgap of 16 mm which is the operational distance between the bearing plates. We did the simulations in different increments, the idea was to map the influence of the segmentation at different levels. The simulations with a small step (1 degree) were performed to try to map the influence within the width of a magnet. We found from the simulations that the influence of the segmentation on the axial force as the bearing rotates is very small. The average force obtained in all the 38 simulations was 12.5589 kN, the maximum force simulated was 12.55974 kN and the corresponding minimum was 12.53914 kN. We found that maximum variation from the average was a bit more than 30 N. The results of the simulations are shown in Fig. 9.

In order to be able to compare the results from the finite element simulations, we also measured the relative movement between the shaft at rated speed and the force through the load cells, the results of these measurements are shown in Fig. 10. From the measurements of force we can see that the obtained thrust force peak oscillations were roughly double than the simulated values. Still, the figures were quite low compared to the operational thrust. In the distance measurements, sharp peaks can be appreciated, they corresponded to four equidistant holes in the measured surface. They were useful to measure the rotational position. From this measurements a pattern can be appreciated, the distance between the plates variated periodically with the rotational frequency. The measured variation was small, the measured peak was less than a fifth of a millimeter.
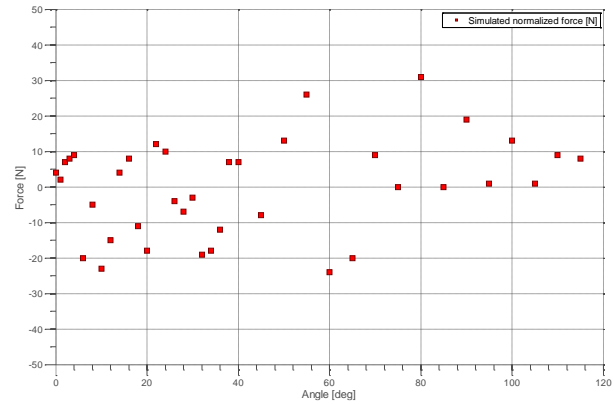

Fig. 9. Simulated normalized force obtained from static three dimensional simulations. As it can be seen in the figure, the expected variation in the force as the bearing rotates is very low compared to the actual carried force of 12.55 kN.
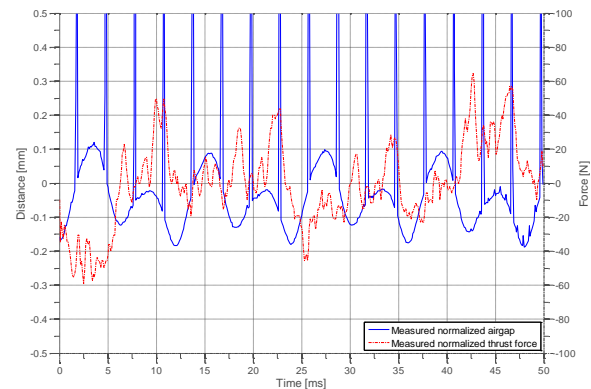

Fig. 10. Normalized measurements of airgap and thrust force at rated speed.

IV. CONCLUSIONS

The results presented in this paper showed that the design, construction and installation of a permanent magnet thrust bearing useable for rotor weights up to a couple of tons is technically feasible. For practical reasons, we decided to build a segmented structure. For the weight required, there were practically no constrains in terms of space, this allowed us to have a comfortable design that resulted in a bearing with a large airgap. Nevertheless, we took provisions to reduce the axial force ripple as much as possible in spite of the segmentation of the magnetic material utilized. The efforts resulted in relatively low axial oscillations. The expected thrust force and the expected ripple due to the segmentation of the magnetic material were simulated utilizing three dimensional finite element calculations. The calculated values had good correspondence with measured ones. The bearing presented in this paper will allow the further investigation magnetic bearings. The simulation tools

verified in this work, will allow us to design larger bearings.

ACKNOWLEDGMENT

REFERENCES

[1] T. Nakata, "Magnetic thrust bearings," *Fuji Denki Review*, vol. 4, no. 2, 1958.

[2] Voith, "Modernization of Europe's largest solution," *HyPower*, no. 2, pp. 38-41, 2002.

[3] M. Nässelqvist, R. Gustavsson, and J. Aidanpää, "Resonance problems in vertical hydropower unit after turbine upgrade," *IAHR 24th Symposium on Hydraulic Machinery and Systems*, Foz do Iguaçu, Brazil, Oct. 2008.

[4] R. Ong, J. H. Dymond, R. D. Findlay, and B. Szabados, "Shaft current in AC induction machine – An online monitoring system and prediction rules," *IEEE Transaction on Industry Applications*, vol. 37, no. 4, 2001.

[5] A. Bonett and G. C. Soupkup, "Cause and analysis of stator and rotor failures in three-phase squirrel-cage induction motors," *IEEE Trans. Ind. Applicat.*, vol. 28, pp. 921-936, 1992.

[6] Y. I. Baiborodov, A. V. Tereshchenko, A. E. Aleksandrov, V. S. Shchetkin, I. B. Pokrovskii, V. P. Tukmakov, and I. S. Gurbanov, "Results of full-scale tests of the thrust bearing with elastic metal-plastic segments for the turbine-generator unit at the Bratsk hydroelectric station," Hydrotechnical Construction, 16: 348, 1982. doi:10.1007/BF02116888

[7] K. Yamaishi, "Applications and performance of magnetic bearing for water turbine generator," *Proceedings of MAG '97, Industrial Conference and Exhibition on Magnetic Bearings*, Virginia, USA, Aug. 1997.

[8] H. Ma, Q. Wang, and P. Ju, "Study of the load reduction for hydrogenerator bearing by hybrid magnetic levitation," *International Journal of Applied Electromagnetics and Mechanics*, no. 43, pp. 215-226, 2013.

[9] M. Wallin, M. Ranlöf, and U. Lundin, "Design and construction of a synchronous generator test setup," *XIX International Conference on Electrical Machines – ICEM*, Rome, Italy, Sep. 2010.

[10] J. K. Nøland, F. Evestedt, J. J. Pérez-Loya, J. Abrahamsson, and U. Lundin, "Design and characterization of a rotating brushless PM exciter for a synchronous generator test setup," *International Conference on Electrical Machines 2016 (ICEM'16)*, 2016.

[11] J. Abrahamsson, "Kinetic Energy Storage and Magnetic Bearings for Vehicular Applications," Ph.D. Dissertation, Uppsala, 2014.

[12] J. Kumbernuss, C. Jian, J. Wang, H. X. Yang, and W. N. Fu, "A novel magnetic levitated bearing system for vertical axis wind turbines (VAWT)," *Applied Energy*, vol. 90, pp. 148-153, 2012.

[13] J. J. Pérez-Loya, J. de Santiago, and U. Lundin, "Construction of a permanent magnet thrust bearing for a hydropower generator test setup," *1st Brazilian Workshop on Magnetic Bearings – BWMB*, Rio de Janeiro, Brazil, Oct. 2013.

[14] J. J. Pérez-Loya and U. Lundin, "Optimization of force between cylindrical permanent magnets," *Magnetics Letters, IEEE*, vol. 5, pp. 1-4, 2014.

[15] Arnold Magnetic Technologies, "Neodymium-Iron-Boron Magnet Grades Summary Product List & Reference Guide," Arnold Magnetic Technologies Corp., 2015. [Online]. Available: http://www.arnoldmagnetics.com/Portals/0/Files/Catalogs%20and%20Lit/Neo/151021/Catalog%20-%20151021.pdf?ver=2015-12-07-103821-497

J. J. Pérez-Loya received the B.Sc. degree in Mechanical and Electrical Engineering from ITESM, Monterrey, Mexico, in 2006, and the M.Sc. degree in Electric Power Engineering from the Chalmers University of Technology, Gothenburg, Sweden, in 2010. Since 2011, he has been working towards the Ph.D. degree in Engineering Physics at Uppsala University, Uppsala, Sweden. He spent 3 years at Ingeniería de Control y Potencia (ICP), Mexico, where he gained industrial experience in water and electricity distribution. His research interest includes the utilization of magnetic forces in electrical machines.

C. J. D. Abrahamsson received the Ph.D. degree in Engineering Physics from Uppsala University, Uppsala, Sweden, in 2014. From 2002 to 2008, he held different positions at ABB, Ludvika, Sweden and Baden, Switzerland, with tasks ranging from research to management. His research interests include scientific simulation, field theory, magnetic bearings, and electric drivelines. Since 2014, he is a Researcher at the Division of Electricity at Uppsala University.

F. Evestedt received the M.Sc. degree in Renewable Electricity Production from Uppsala University, Uppsala, Sweden, in 2015. He is currently working towards the Ph.D. degree in Engineering Physics at Uppsala University, Uppsala, Sweden. His research interest include electronics, power electronics, measurement circuits and PCB design.

U. Lundin received the Ph.D. degree in Condensed Matter Theory from Uppsala University, Uppsala, Sweden, in 2000. From 2001 to 2004, he was a Postdoctoral at the University of Queensland, Brisbane, Australia. In 2004, he joined the Division for Electricity at Uppsala University where he is currently Professor in Electricity with specialization towards Hydropower Systems. His research focuses on synchronous generators and their interaction with mechanical components and the power system. He leads the Hydropower Group and has been involved in the industrial implementation of research projects. His current research interests include excitation systems and magnetic bearings.